Magnetic Compton scattering study of the magnetocaloric material Gd_7Pd_3

2007 J. Phys.: Condens. Matter 19 186208

(http://iopscience.iop.org/0953-8984/19/18/186208)

J. Phys.: Condens. Matter **19** (2007) 186208 (7pp) doi:10.1088/0953-8984/19/18/186208

Magnetic Compton scattering study of the magnetocaloric material Gd_7Pd_3

C Shenton-Taylor[1], J A Duffy[1], J W Taylor[2], C A Steer[1], D N Timms[3], M J Cooper[1] and L V Blaauw[1]

[1] Department of Physics, University of Warwick, CV4 7AL, UK
[2] ISIS, RAL, Chilton, Didcot, Oxfordshire OX11 0QX, UK
[3] School of Earth and Environmental Sciences, University of Portsmouth, Portsmouth PO1 3QL, UK

Received 19 January 2007, in final form 11 March 2007
Published 5 April 2007
Online at stacks.iop.org/JPhysCM/19/186208

Abstract

The spin-dependent momentum density of Gd_7Pd_3 was probed by the magnetic Compton scattering technique with elliptically polarized synchrotron radiation. A contribution to the spin moment from Pd 4d electrons was observed, at 2 and 280 K, alongside a large Gd 4f moment and a smaller Gd 5d moment. The total spin moment, at 2 K, was determined as $50.8 \pm 0.7\ \mu_B$ (f.u.)$^{-1}$. The Gd 4f contribution to the spin moment was determined as $43.4 \pm 1.8\ \mu_B$ (f.u.)$^{-1}$, the Gd 5d moment as $4.4 \pm 0.7\ \mu_B$ (f.u.)$^{-1}$ and the Pd 4d spin moment contribution as $2.9 \pm 1.1\ \mu_B$ (f.u.)$^{-1}$, where f.u. represents a formula unit. At 280 K the total spin moment was $27.3 \pm 0.9\ \mu_B$ (f.u.)$^{-1}$ with individual contributions determined as a Gd 4f spin moment of $23.8 \pm 1.1\ \mu_B$ (f.u.)$^{-1}$, a Gd 5d contribution of $2.2 \pm 0.5\ \mu_B$ (f.u.)$^{-1}$ and a Pd 5d spin moment of $1.2 \pm 0.6\ \mu_B$ (f.u.)$^{-1}$.

1. Introduction

Magnetic refrigeration is evolving as a potential competitor to the existing refrigeration technology, as reviewed by Brück [1]. If developed it could offer several advantages, including more compact devices as the working material is a solid, higher thermodynamic efficiency, and absence of ozone-depleting chlorinated fluorocarbons [2, 3]. The exploitation of the magnetic refrigeration process requires materials possessing near-room-temperature magnetocaloric properties. The magnetocaloric effect is a well known physical effect [4]; under the influence of an external magnetic field, whilst under adiabatic conditions, a change in temperature of the magnetic material can be induced [5]. Accompanying the discovery of the giant magnetocaloric effect in $Gd_5Ge_2Si_2$, there has been an increased drive to identify materials with near-room-temperature magnetocaloric properties, preferably with higher transition temperatures and therefore better cooling capacities [6, 7].

The material Gd_7Pd_3 is an intermetallic compound, which crystallizes in the Th_7Fe_3 structure type [8, 9], and orders ferromagnetically above room temperature ($T_C = 323$ K). Recently, Talik *et al* [10] have published a comprehensive study of its structural, electronic and magnetic properties. A study of the magnetocaloric properties, conducted by Canepa *et al* [11], used heat capacity measurements to calculate the isothermal entropy change, ΔS_M, and the adiabatic temperature rise, ΔT_{ad}, in magnetic fields of 2 and 5 T at 320 K. The normalized parameters, $\Delta S_M/\Delta H$ and $\Delta T_{ad}/\Delta H$, where ΔH is the enthalpy, enable comparison of Gd_7Pd_3 against known materials which order at a similar temperature. Comparing these quantities, Gd_7Pd_3 shows surprisingly high and useful values. For Gd_4Bi_3 $\Delta S_M/\Delta H = -5.3$ mJ cm^{-3} K^{-1} T^{-1} whilst the preferred magnetic refrigeration material $Gd_5Ge_{2.5}Si_{1.5}$ is much higher at -14.1 mJ cm^{-3} K^{-1} T^{-1}; in comparison Gd_7Pd_3 is nearer this value, with -11.3 mJ cm^{-3} K^{-1} T^{-1} [11]. The high ferromagnetic ordering temperature and appropriate values of $\Delta S_M/\Delta H$ and $\Delta T_{ad}/\Delta H$ promote Gd_7Pd_3 as a serious candidate for magnetic refrigeration. The limitation is the expense of Pd, which at present prevents industrial applications.

In this study, magnetic Compton scattering has been used to investigate the bulk magnetic spin density of Gd_7Pd_3 and to estimate the contributions from the Gd 4f, Gd 5d and Pd 4d moments. Magnetic Compton scattering was used to probe the spin-density momentum at both 2 and 280 K, with external magnetic fields of 6 and 5 T respectively.

2. Magnetic Compton scattering

Magnetic Compton scattering is an established technique for probing momentum-space spin densities and band structures in magnetic materials [12]. Within the impulse approximation the method is solely sensitive to the spin magnetic moments; the orbital moment is not measured. A further advantage is that magnetic Compton scattering has uniform sensitivity to the whole of the spin-dependent electron momentum distribution.

The Compton profile is defined as the one-dimensional projection of the electron momentum distribution, $n(\boldsymbol{p})$,

$$J(p_z) = \int\int n(\boldsymbol{p})\,\mathrm{d}p_x\,\mathrm{d}p_y. \tag{1}$$

By convention, $J(p_z)$ is the total number of electrons per formula unit. The profile is obtained experimentally from the inelastic scattering of mono-energetic photons though a fixed angle. Scattering from the moving electrons leads to a Doppler broadened energy distribution. The direct relation between the distribution of the Compton profile and the double differential scattering cross section enables the spin moment to be isolated. A derivation of the inelastic scattering cross section is described by Bell *et al* [13].

The magnetic Compton profile arises from the difference between the electrons in the spin-up and spin-down bands. A small spin-dependent term appears in the scattering cross section if the photons have a component of circular polarization. The spin term can be isolated by changing the direction of the sample's magnetization, or the polarization of the photons. The spin-dependent term will change sign, whilst the charge scattering component remains unaltered. On subtraction of two Compton profiles the charge contribution will cancel, leaving only the magnetic term. The isolated spin-dependent term leads to $J_{mag}(p_z)$, known as the magnetic Compton profile (MCP). The resulting MCP is the twice-integrated spin-dependent momentum density,

$$J_{mag}(p_z) = \int\int (n\uparrow(\boldsymbol{p}) - n\downarrow(\boldsymbol{p}))\,\mathrm{d}p_x\,\mathrm{d}p_y \tag{2}$$

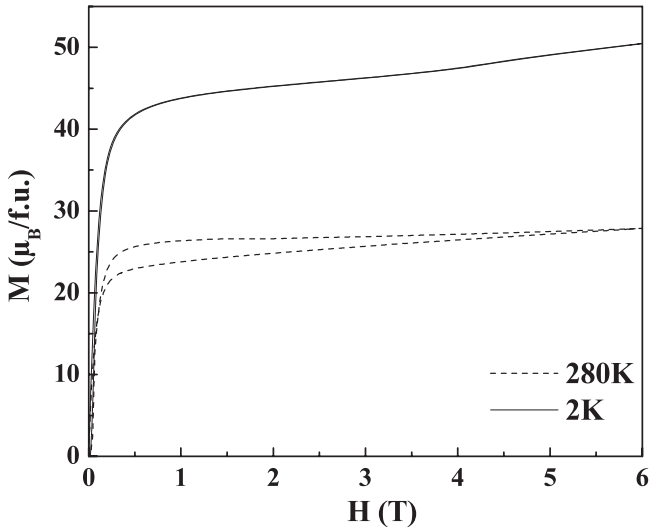

Figure 1. VSM magnetization data as a function of external magnetic field of Gd_7Pd_3. At near room temperature, hysteresis is present.

where $n\uparrow(\boldsymbol{p})$ and $n\downarrow(\boldsymbol{p})$ are the momentum-dependent spin densities for the majority and minority bands, respectively. Adopting the same normalization criterion as in equation (1), the area under the MCP is equal to the total spin moment per formula unit, i.e. the number of unpaired electrons.

$$\int_{-\infty}^{\infty} J_{\mathrm{mag}}(p_z)\,\mathrm{d}p_z = \mu_{\mathrm{spin}}. \tag{3}$$

Relativistic Hartree–Fock (RHF) free-atom profiles [14] were used to compare the experimental Gd_7Pd_3 MCPs to those predicted from theory. The RHF free-atom profiles accurately describe the inner-shell electrons, such as those in the Gd 4f orbital [12].

3. Experimental details

Polycrystalline samples of Gd_7Pd_3 were prepared by arc-melting, using a water-cooled copper hearth in an argon atmosphere, starting with the appropriate concentrations of constituent elements. The purity of the starting constituents were 99.99% mass fraction or better of palladium granules and 99.9% mass fraction or better of gadolinium chips. To ensure good homogeneity, the resulting alloy button was flipped and remelted several times. The structure of the sample was characterized by electron dispersive x-ray analysis (EDAX). From back-scattered images three phases were identified in the sample, with the overall composition ratio Gd:Pd of 7:3.

Magnetization measurements were carried out on a vibrating sample magnetometer (VSM) with fields up to 6 T and temperatures down to 2 K. The data, shown in figure 1, show a rapid change in magnetic moment up to 0.5 T, after which the moment starts to saturate. At temperatures near room temperature, hysteresis is observed. At 2 K and 6 T the VSM measurement of the total moment was $50.5\pm2.0\ \mu_{\mathrm{B}}$ (f.u.)$^{-1}$, reducing to $27.5\pm1.1\ \mu_{\mathrm{B}}$ (f.u.)$^{-1}$ at 280 K and 5 T.

The MCPs were measured on a high-energy x-ray beamline (ID15) at the ESRF, Grenoble. The experiment was performed in a reflection geometry with an incident beam energy of

Table 1. Magnetic moments, in Bohr magnetons per formula unit, μ_B (f.u.)$^{-1}$, of Gd_7Pd_3 as a function of temperature.

Temperature (K)	Spin moment μ_B (f.u.)$^{-1}$	Estimated Gd 4f spin moment μ_B (f.u.)$^{-1}$	Estimated Gd 5d spin moment μ_B (f.u.)$^{-1}$	Estimated Pd 4d spin moment μ_B (f.u.)$^{-1}$
2	50.8 ± 0.7	43.4 ± 1.8	4.4 ± 0.7	2.9 ± 1.1
280	27.3 ± 0.9	23.8 ± 1.1	2.2 ± 0.5	1.2 ± 0.6

167 keV. The energy distribution of the scattered x-rays was measured by a 13-element solid-state Ge detector, of which 12 elements were operational. The sample was contained within the poles of a cryomagnet and the magnetization was periodically reversed. At 2 K the MCP was produced by reversing a 6 T magnetic field; a 5 T magnetic field was reversed at 280 K. The momentum resolution of the measurement was 0.44 au (where 1 au $= 1.99 \times 10^{-24}$ kg m s^{-1}). This resolution was dominated by the intrinsic resolution component of the detector with small contributions arising from the monochromator bandwidth and a geometrical contribution. This resolution has proved suitable for quantitative analysis of experimental MCPs in numerous investigations. The data were corrected for detector efficiency and for absorption in the sample. The spin-dependent relativistic scattering cross section of Bell *et al* [13] was used to relate the measured scattered photon energies to the electron momentum density. Corrections for magnetic multiple scattering, performed following the procedure of Felsteiner *et al* [15], were found to be insignificant compared to the statistical accuracy of the data. The resultant profiles were symmetric about zero momentum, as they should be if the corrections have been properly applied. To increase the statistical precision of the data the MCPs were folded about zero.

4. Magnetic Compton scattering results

The experimental Gd_7Pd_3 MCPs at 2 and 280 K are presented in figures 2(a) and (b) respectively. In both cases the data are fitted to an RHF free-atom Compton profile comprising of contributions from the Gd 4f, Gd 5d and Pd 4d unpaired electrons. The inclusion of a small Pd 4d contribution lifts the low-momentum region, thereby improving the correlation between the RHF free-atom fit and the experimental data. The individual RHF free-atom fits, convoluted with an experimental resolution of 0.44, for Gd 4f, Gd 5d and Pd 4d are also shown in figure 2.

5. Spin moment analysis

The areas under the modelled Gd 4f, Gd 5f and Pd 4d RHF profiles give the related spin moments, as shown in table 1, where the random errors are estimated from the statistical error in the MCP data points. Detailed interpretation of delocalized electron bands would require electronic band structure calculations. However, the overall momentum distribution of the contributions to the spin moment should match those predicted by RHF free-atom profiles. Hence the experimentally obtained MCP can be decomposed into shell and site-specific contributions by the simple addition or subtraction of the relevant inner-shell-specific lineshapes.

By dividing the overall spin moment, taken from the VSM measurement, into the ratio of Gd 4f, Gd 5d and Pd 4d, as used in the Hartree–Fock profile, the individual contributions can be estimated. As would be expected, at both 2 and 280 K the major contribution to the spin moment is from Gd 4f electrons. At 2 K the Gd 4f moment is estimated as 43.4 ± 1.8 μ_B per formula unit, (f.u.)$^{-1}$. This is less than the saturated value, of 49 μ_B (f.u.)$^{-1}$, since

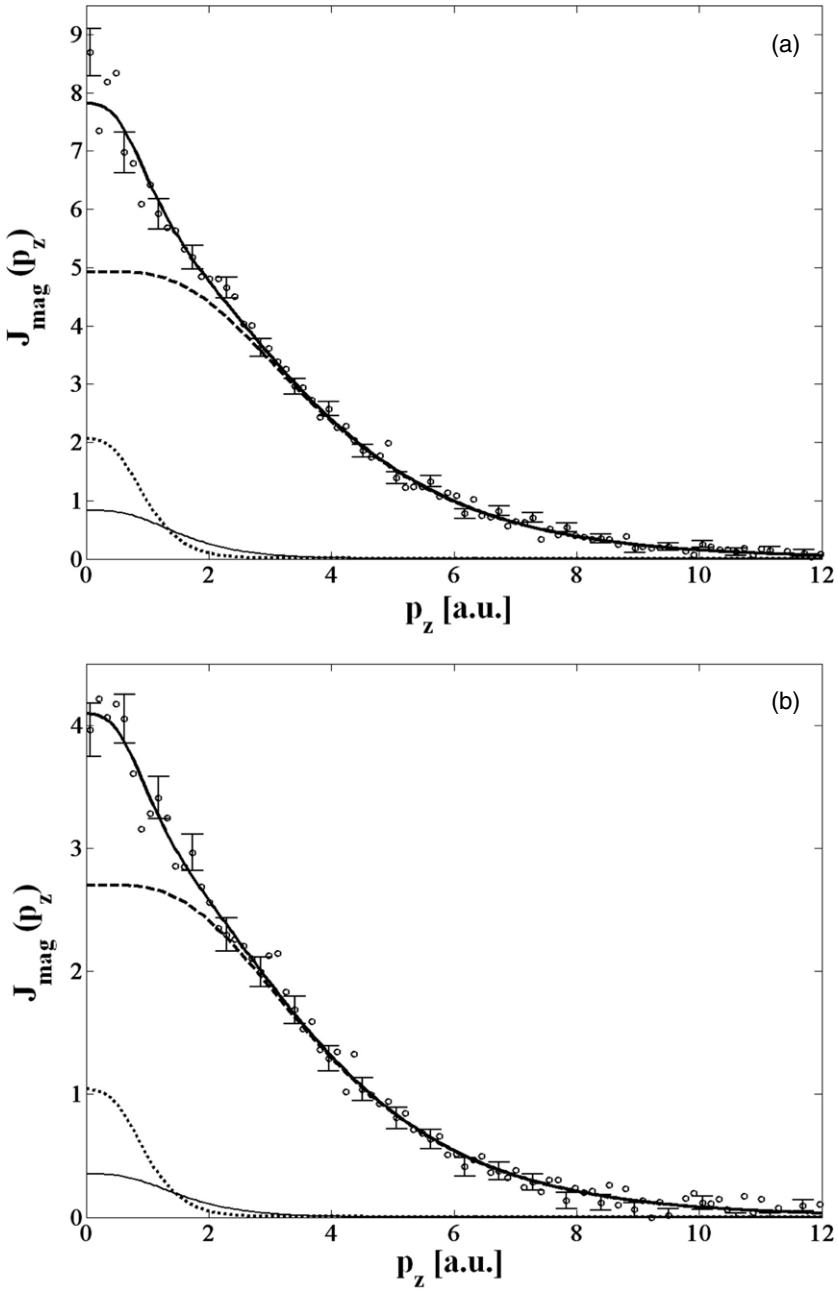

Figure 2. (a) MCP of Gd_7Pd_3 at 2 K folded about zero momentum. The data are described by an RHF free-atom fit (——) comprising a large Gd 4f spin moment (- - - -) and smaller contributions from a Gd 5d (· · · · · ·) and a Pd 4d (——) moment. (b) MCP of Gd_7Pd_3 at 280 K, folded about zero momentum. Again, RHF free-atom fits of a Gd 4f moment (- - - -), Gd 5d moment (· · · · · ·) and a Pd 4d moment (——) are shown, combining to give a total profile (——) that describes the 280 K profile.

at the temperature and field used, the magnetization itself has not been saturated. The 4f moments decreases to $23.8 \pm 1.1\ \mu_B$ (f.u.)$^{-1}$ at 280 K. A small Gd 5d contribution is observed,

estimated as $4.4 \pm 0.7\ \mu_B$ (f.u.)$^{-1}$ at 2 K, decreasing to $2.2 \pm 0.5\ \mu_B$ (f.u.)$^{-1}$ at 280 K. The Gd 5d spin polarization at low temperature, corresponding to $0.6 \pm 0.1\ \mu_B$ per Gd atom, is consistent with that observed in pure Gd [12]. In order to fit to the data, a Pd 4d contribution is required at both temperatures, estimated as $2.9 \pm 1.1\ \mu_B$ (f.u.)$^{-1}$ at 2 K, decreasing to $1.2 \pm 0.6\ \mu_B$ (f.u.)$^{-1}$ at 280 K. At low temperature this corresponds to 1 μ_B per Pd atom. We believe that this Pd moment is induced by the Gd magnetization. In the applied fields used in this study, pure Pd would have a much smaller magnetic moment, of around $10^{-3}\ \mu_B$ per Pd atom [16, 17]. Furthermore, it is known that large Pd moments can be induced when small amounts of ferromagnetic impurities are added; for examples see Constant *et al* and Crangle *et al* [18, 19]. Given the localized nature of the Gd 4f orbitals, it seems likely that the Pd moment observed in Gd_7Pd_7 is probably induced via hybridization with the itinerant Gd 5d electrons, which carry a moment as described above.

The spin moment can also be found from the flipping ratio by comparing the magnitudes of the MCP with the charge profile and with knowledge of the degree of circular polarization of the beam. At 280 K the overall moment was estimated as $27.3 \pm 0.9\ \mu_B$ (f.u.)$^{-1}$, in good agreement with the VSM measurement of $27.5 \pm 1.1\ \mu_B$ (f.u.)$^{-1}$. At 2 K the charge profile will have scattering contributions from both the sample and liquid helium, and we estimated that 40% of the charge profile is scattering from sources other than the sample. Including this factor, the flipping ratio gives an overall moment of $50.8 \pm 0.7\ \mu_B$ (f.u.)$^{-1}$, which agrees with the VSM measurement of $50.5 \pm 2.0\ \mu_B$ (f.u.)$^{-1}$. These values for the total spin moment, which are not model dependent, show no evidence for the existence of an orbital magnetic moment.

Because the Pd 4d and Gd 5d electrons are not localized, a more accurate profile shape could be achieved from band structure calculations which could alter the estimated contributions. However, it is worth noting that band structure calculations would not produce fits with widths very different from those calculated by Hartree–Fock methods. In particular, the MCPs measured at 2 and 280 K both require finite Pd 4d moment contributions to fit the width of the profile in the momentum distribution range 2–4 au.

6. Conclusions

In conclusion, the magnetic Compton profiles show a contribution to the spin moment from Gd 4f, Gd 5d and Pd 4d. There is also expected to be a small contribution from a Gd 6s moment at very low momentum. Hartree–Fock free atom profiles have been used to successfully model the measured MCPs. The free-atom model will impact on the magnitude of the estimated spin moment contributions; however, in order to model the Compton lineshape only Pd 4d electrons have the characteristic momentum density distribution required. The moment is dominated by a Gd 4f contribution, with a smaller moment from Gd 5d and Pd 4d. We estimate the Pd 4d contribution as $2.9 \pm 1.1\ \mu_B$ (f.u.)$^{-1}$ at 2 K decreasing to $1.2 \pm 0.6\ \mu_B$ (f.u.)$^{-1}$ at 280 K. We emphasize the need for a small Pd 4d moment in order to model the MCPs measured in this experiment.

Acknowledgments

We thank the ESRF for allocation of beamtime and the EPSRC for generous financial support under grant GR/S44211/1. We would like to thank Veijo Honkimäki, Thomas Buslaps and the staff of ID15 for their help and support.

References

[1] Brück E 2005 *J. Phys. D: Appl. Phys.* **38** R381
[2] Tegus O, Brück E, Buschow K H J and de Boer F R 2002 *Nature* **415** 150

[3] Glanz J 1998 *Science* **279** 2045
[4] Warburg E 1881 *Ann. Phys. Chem.* **13** 141
[5] Gschneidner K A Jr, Pecharsky V K and Tsokol A O 2005 *Rep. Prog. Phys.* **68** 1479–539
[6] Provenzano V, Shapiro A J and Shull R D 2004 *Nature* **429** 85
[7] Gschneidner K A and Pecharsky V K 1999 *J. Appl. Phys.* **85** 8
[8] Berkowitz A E, Holtzberg F and Methfessel S 1964 *J. Appl. Phys.* **35** 1030
[9] Moreau J M and Pathé E 1973 *J. Less-Common Met.* **32** 91
[10] Talik E, Klimczak M, Troć R, Kusz J, Hofmeister W and Damm A 2007 *J. Alloys Compounds* **427** 30
[11] Canepa F, Napoletano M and Salvino C 2002 *Intermetallics* **10** 731–4
[12] Duffy J A, McCarthy J E, Dugdale S B, Honkimäki V, Cooper M J, Alam M A, Jarlborg T and Palmer S B 1998 *J. Phys.: Condens. Matter* **10** 10391
[13] Bell F, Felsteiner J and Pitaevskii P L 1996 *Phys. Rev.* A **53** R1213
[14] Biggs F, Mendelsohn L B and Mann J B 1975 *At. Data Nucl. Data Tables* **16** 201
[15] Felsteiner J, Pattison P and Cooper M J 1974 *Phil. Mag.* **30** 537
[16] Jamieson H C and Manchester F D 1972 *J. Phys. F: Met. Phys.* **2** 323
[17] Foner S and McNiff E J Jr 1967 *Phys. Rev. Lett.* **19** 1438
[18] Constant F W 1930 *Phys. Rev.* **6** 1654
[19] Crangle J 1960 *Phil. Mag.* **5** 335